

HYDROLOGY DOCUMENT NUMBER 617

Hydrogeologic impacts of mine design in unsaturated rock

R. E. Williams, S. D. Vincent and G. Bloomsburg

Abstract—A modeling scheme is developed to simulate the hydrogeologic effects of mine design and development in unsaturated rock. Simulations are conducted using the UNSAT2 finite element computer program and hydrogeologic data from the site of a proposed mined-out waste repository at Yucca Mountain, NV. Results of the simulations are analyzed for:

- variations in the direction of ground water flow and in the distribution of pressure head caused by the design of the mined out openings; and

- mine design variables that affect the predicted rates of mine water inflow.

Evaluating the hydrogeologic impacts of mine design and mine development in unsaturated rock is significant in several respects. Characterization of the preemplacement of wastes along the fastest path ground water flow system at the Yucca Mountain site has been a primary research effort. Ultimately, however, the degree to which waste isolation is achieved will depend largely on the post-mining hydrogeologic environment as altered by the mine design and on the radionuclide inventory and resulting heat effects of the repository. Therefore, an ongoing characterization of the proposed mined-out nuclear waste repository at Yucca Mountain, NV, is recommended. Modeling results indicate that:

- mined out openings will affect the movement of ground water, both in rate and direction;

- hydraulic effects of mine development depend on the hydrogeologic environment and on mine design geometry;

- mine water inflow is possible in the unsaturated zone, even for mines developed in hydrogeologically homogeneous rocks; and

- mine water inflow can occur at values of downward flux that are appreciably less than the saturated hydraulic conductivity of the overlying rocks.

Introduction

Yucca Mountain, NV, is a candidate site for a proposed mined-out geologic repository for the disposal of high-level radioactive waste. The proposed repository horizon is in unsaturated rocks of the Topopah Spring Member of the Paintbrush Tuff formation. The Topopah Spring Member at Yucca Mountain consists of several fractured, densely welded ash-flow sheets (Department of Energy, 1986).

A conceptual model of the existing unsaturated flow system at Yucca Mountain is presented by Montazer and Wilson (1984). Their model assumes steady downward flow in the matrix. Based on unsaturated flow theory, this conceptual model envisions no water flow in open fractures if the vertical liquid flux is less than the saturated matrix hydraulic conductivity of the tuff. Available data indicate that the flux through the repository horizon is less than the mean saturated matrix hydraulic conductivity (Department of Energy, 1986).

Bloomsburg et al., (1989) demonstrated that spatial variations in the hydraulic properties (hydrogeologic heterogeneities) of a porous rock matrix cause flux to be distributed nonuniformly in space. In the case of Yucca Mountain, heterogeneities in the tuff may cause zones to develop in which the flux is greater than the saturated matrix hydraulic conductivity.

In this scenario, positive water pressures (pressures greater than atmospheric) develop where matrix conductivity is exceeded by the flux, thereby allowing water to enter and flow through open fractures.

Subsurface mining can be envisioned as the creation of a hydrogeologic heterogeneity. As such, constructing a repository at Yucca Mountain might be expected to cause flux to be distributed non-uniformly by reducing the cross-sectional area available for vertical flow through the host rock. Potential impacts of this condition include:

- the initiation of fracture flow accompanied by a reduced ground water travel time through the unsaturated zone; and

- unanticipated inflow of water to the repository under positive pressure during construction and operation.

The research presented here uses a numerical model to assess the hydrogeologic impacts of mine design and development in unsaturated rocks.

The simulation of the flow in the matrix was accomplished with the finite element computer program UNSAT2 (Davis and

R.E. Williams, member SME, is professor of hydrogeology and director, Waste Management Studies, College of Mines and Earth Resources, University of Idaho, Moscow, ID. S.D. Vincent is a hydrogeologic consultant, Boise, ID. G. Bloomsburg is professor of agriculture engineering, College of Agriculture, University of Idaho, Moscow, ID. SME nonmeeting paper 89-238. Manuscript November 1989. Discussion of this paper must be submitted, in duplicate, prior to Dec. 31, 1990.

Neuman, 1983). This uses the Richard's equation and a Galerkin type finite element formulation to simulate unsteady, partially saturated flow. The program will simulate irregular boundaries with seepage surface, constant flux and constant potential conditions. The seepage surface condition is needed to model mine water inflow in the vadose zone (Williams et al., 1986) while simulation of realistic mine design geometries requires irregular boundaries.

The theoretical aspects of UNSAT2 and other examples of its use are presented by Davis and Neuman (1983), by Williams et al., (1986) and by Bloomsburg et al., (1989).

Model construction

A vertical section of the Paintbrush Tuff formation at Yucca Mountain is presented by Bloomsburg et al., (1989). The principal reasons for selecting the rocks of the Topopah Spring Member of the Paintbrush Tuff for study are:

- the mined out waste repository is proposed for development in this tuff unit; and
- these rocks have been tested for both saturated and unsaturated hydraulic properties.

The saturated hydraulic conductivity was measured whereas the unsaturated conductivity was calculated from mercury intrusion and pressure plate data by the methods of Maulem (1976) and Van Genuchten (1980), as reported in Peters et al., (1984). The data used in simulation were from sample G4-5 that was assumed to be representative of the Topopah Spring Member. A single sample value for saturated conductivity was used instead of an average value because the unsaturated flow properties were available only for individual samples.

Prototype mine design consists of conventional rooms and pillars. The planned repository is designed on one level that is 200 to 400 m (656 to 1312 ft) above the water table (Department of Energy, 1986) and 285 m (935 ft) below land surface at drillhole USW G-4 (MacDougall, 1984). Figure 1 is a plan view of one of two alternative proposed designs. The dominant geometric feature of both designs is a series of equally spaced and parallel waste emplacement drifts located roughly along a horizontal plane.

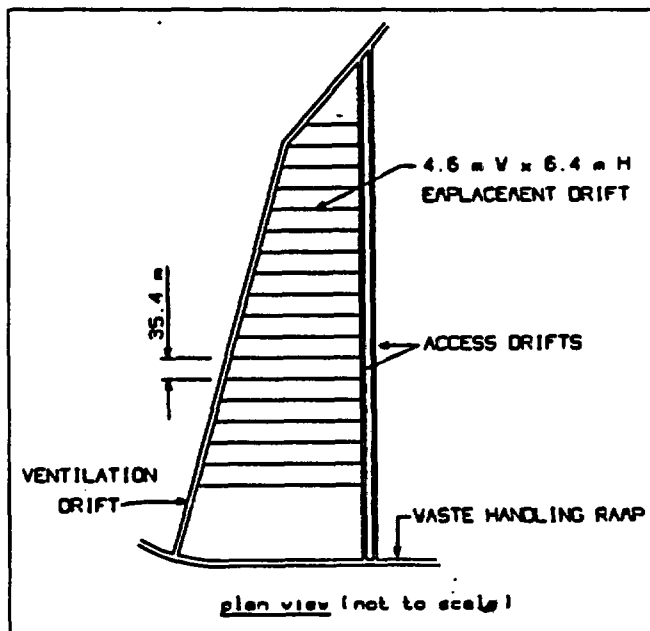


Fig. 1 — Stage 1 repository development plan for Yucca Mountain, NV (after MacDougall, 1984).

The modeling scheme incorporates symmetry principles to model downward (not vertical) flow through a homogeneous vertical section. This section intersects equally spaced, horizontal and parallel drifts, although the repository will be slightly inclined (Fig. 2).

Vertical planes of symmetry, between and bisecting drifts, are treated as zero-flux boundaries. The water table is treated as a fixed atmospheric pressure boundary. The upper boundary reflects uniform, constant flux that can be changed between simulations. Mined-out regions are modeled as seepage surfaces that are considered external boundaries in UNSAT2.

Mine design variables tested were the spacing of drifts, the height and width of drifts and the shape of drift backs (roofs), along with the magnitude of the flux. Different mesh configurations were analyzed while maintaining similar element shapes, sizes and positions in the simulated mine because finite element analyses can be affected by changes in spatial discretization.

The mesh

The details of mesh construction for this work are presented in Vincent (1989). The mesh reflects homogeneous and isotropic rock with the hydraulic properties of sample G4-5. Figure 3 illustrates that the elevation above the water table at which pressure head becomes invariant increases with decreasing flux. To identify the elevation where invariant pressure heads occur, steady downward flow was simulated with a trial mesh using the lowest value of flux evaluated in this study.

Analysis of the output revealed that the nodal steady-state pressure heads are essentially identical above an elevation of 85 m (279 ft) above the water table. Consequently, all mine openings were placed at least 100 m (328 ft) above the lower

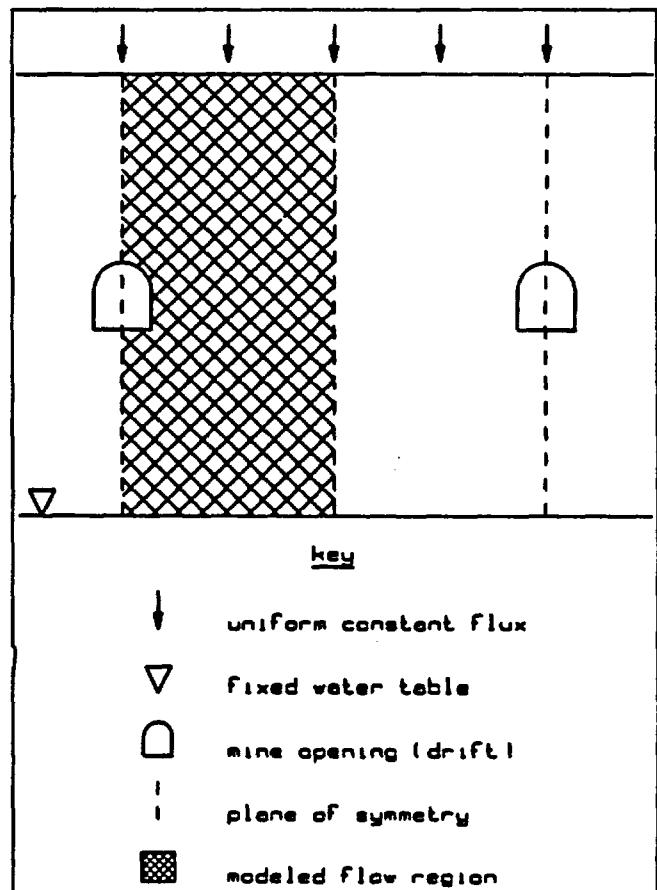


Fig. 2 — Schematic vertical section of typical mine simulation.

boundary (water table). The vertical dimension of all meshes is 200 m (656 ft) to ensure adequate separation from both lower and upper boundaries (Fig. 4). The indented edges of otherwise rectangular meshes are seepage surface boundaries at drift-rock interfaces. Mesh widths correspond to one-half of drift spacing as measured between drift centers.

Geometric similarity in mesh construction was used to isolate the effects of the variables tested from those associated with spatial discretization. Zlamal (1968) showed that solution error for a triangular element is proportional to the square of the length of the longest side of the triangle squared and inversely proportional to the smallest angle.

Consequently, element angles were maximized. Elongated elements were avoided wherever possible. This effort is important because UNSAT2 automatically divides quadrilaterals into triangles. Element dimensions generally are smallest where hydraulic gradients are greatest such as in the vicinity of mine openings (where interest is focused) and near upper and lower boundaries.

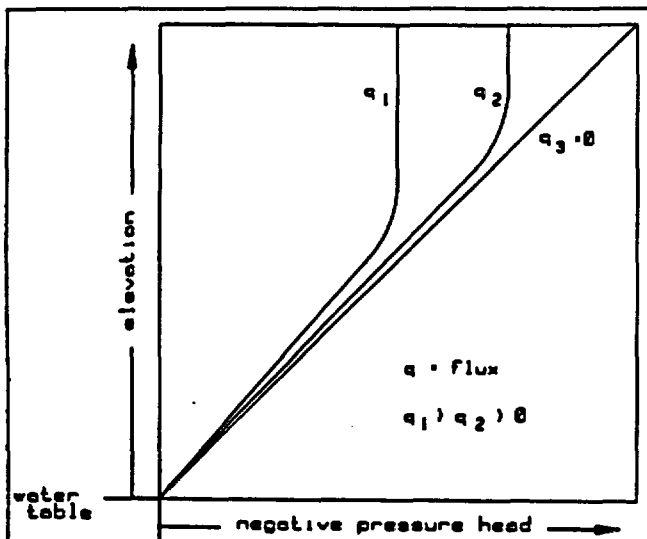


Fig. 3 — General relationship between negative pressure head and elevation above the water table during steady downward flow through a homogeneous rock profile (adapted from Corey, 1986). Not to scale.

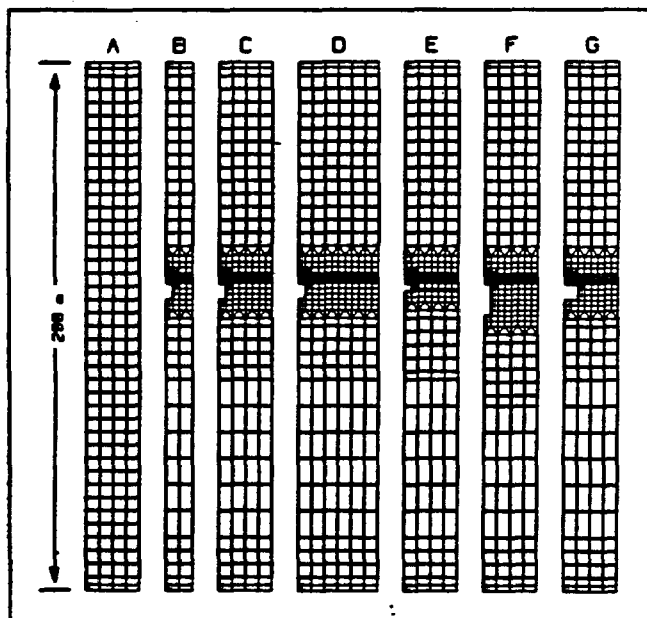


Fig. 4 — Generalized finite element mesh configurations (see text for explanation of horizontal dimension).

Both pre-mining and post-mining scenarios are simulated in order to assess mining-induced changes in ground water flow patterns. Pre-mining flow is simulated using a mesh without drifts (mesh A in Fig. 4). Post-mining flow scenarios are simulated with meshes containing seepage boundaries (mine boundaries) as shown in meshes B through G in Fig. 4. Each of these generalized mesh configurations has three variants that correspond to drift back (roof) slopes of 0°, -10°, and -20° (designated as C0, C10 and C20, respectively). Examples of subconfigurations for mesh C are shown in Fig. 5.

Mesh C20 serves as the prototype from which all other mesh configurations are variations. The drift boundary for mesh C20 was configured to approximate the design shape of the drift in one of the two design plans for the proposed mined repository within Yucca Mountain as shown in Fig. 6. The curved design of the back was approximated with a sloping straight line. The width of mesh C is one-half the drift spacing called for in the repository design.

Drift spacing was varied from mesh C by the addition or deletion of geometrically identical columns of elements. The slope of a drift back was varied by modification of element shapes, as necessary, for elements along and above the section of seepage surface that defines

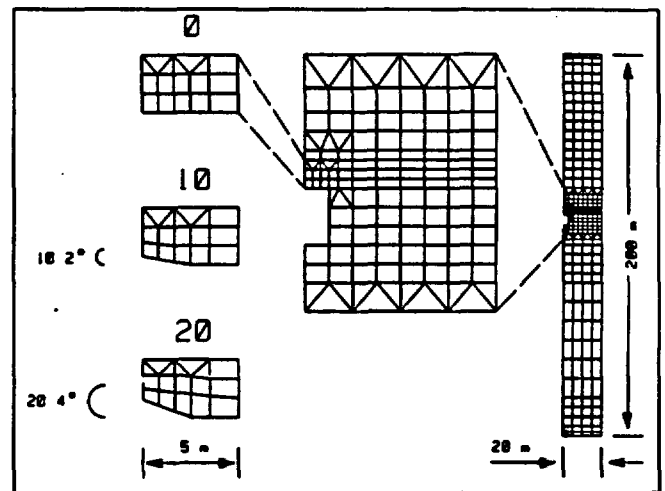


Fig. 5 — Mesh C subconfigurations for drift back slopes of 0°, 10° and 20°.

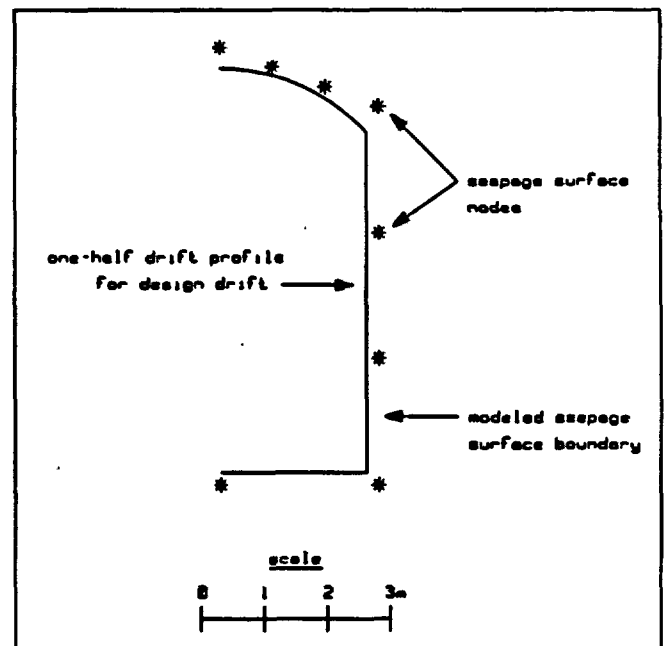


Fig. 6 — Comparison of design drift profile with prototype seepage surface boundary.

the drift back. Altering drift dimensions amounted to expanding or contracting the seepage surface boundary by the addition or deletion of elements. A description of the various mesh configurations used in this study is presented in Table 1.

Mesh Designation	Mesh height (m)	Mesh width (m)	Number of Elements	Number of Nodes	Seepage Boundary Height (m)	Seepage Boundary Width (m)
A	200	20	168	215	N/A	N/A
B	200	10	136	173	6	2.5
C	200	20	256	291	6	2.5
D	200	30	380	409	6	2.5
E	200	20	255	288	3	2.5
F	200	20	279	315	12	2.5
G	200	20	263	295	6	5.0

* meshes B through G have three subconfigurations each for a total of nineteen separate mesh geometries

Hydrologic properties

All meshes are developed for isotropic rocks that have the hydrogeologic properties reported by Peters et al., (1984) for sample G4-5 of the Topopah Spring Member. The average measured saturated hydraulic conductivity for this sample is 0.6 mm/a (0.023 in. per year). The porosity is 0.09 (0.0035).

Relative hydraulic conductivity (effective hydraulic conductivity divided by saturated hydraulic conductivity) as a function of moisture content $[K_r(\theta)]$ and pressure head as a function of moisture content $[h(\theta)]$ are input to UNSAT2 in tabular form. The table for this modeling exercise was produced using curve-fitting parameters presented by Peters et al., (1984) for a van Genuchten (1980) fit of sample G4-5 saturation data. The van Genuchten (1980) curvefitting technique uses the least squares parameter estimation technique of Mualem (1976) and semi-empirical equations that relate moisture content, pressure head and relative hydraulic conductivity. Vincent (1989) presented the details and the results of the application of these techniques to the data for the Yucca Mountain site.

The initial negative pressure conditions for all simulations was set at 1.5 m (5 ft) of water. A negative pressure of 1.5 m (5 ft) corresponds to 99.9% of complete saturation for sample G4-5. The high initial degree of saturation condition was used in order to speed convergence and to reduce the computer time required to achieve steady state.

The upperbound flux for all designs tested is 0.54 mm/a (0.02 in. per year) (90% of the saturated hydraulic conductivity for sample G4-5). Flux successively was decremented from this value by 0.02 mm/a (0.00078 in. per year) for each mesh containing a drift until the rate of mine water inflow reached zero.

Hydrogeologic properties are identical for all simulations in order to isolate the effects of selected geometric variables that correspond to mine design. All simulations were run until steady state conditions were achieved. Steady state is assumed when inflow and outflow rates become essentially equal (less than 2% difference) and unchanging between successive time steps. A total of 145 different combinations of drift design and fluxes were simulated for this study as summarized in Table 2.

Mesh	Flux Range (mm/yr)	Drift Spacing (m)	Drift Height (m)	Drift Width (m)	Drift Back Slopes (°)
A	0.36-0.54	40	N/A	N/A	N/A
B	0.40-0.54	20	6	5	0, 10, 20
C	0.42-0.54	40	6	5	0, 10, 20
D	0.42-0.54	80	6	5	0, 10, 20
E	0.44-0.54	40	3	5	0, 10, 20
F	0.42-0.54	40	12	5	0, 10, 20
G	0.36-0.54	40	6	10	0, 10, 20

Effects of mine design

Impact of a drift

Steady state nodal output was analyzed for:

- changes in the direction of flow and the distribution of pressure head caused by mine openings; and
 - variables that affect the predicted rate of mine water inflow.
- Nodal conditions are described in terms of fluid potential and pressure head.

The effects of mine design and development on ground water flow are assessed by comparing pre-mining flow scenarios simulated with mesh A (Fig. 4) to post-mining flow as simulated with the prototype mesh (C20). These meshes are identical with respect to hydraulic properties and dimensions.

Flow through mesh A is everywhere downward for all flux values because the rocks simulated are homogeneous and the mesh has vertical sides. The flow net is not shown in the figure because the flux direction is everywhere vertical. The homogeneous negative pressure head is about 3.4 m (11 ft) for a flux of

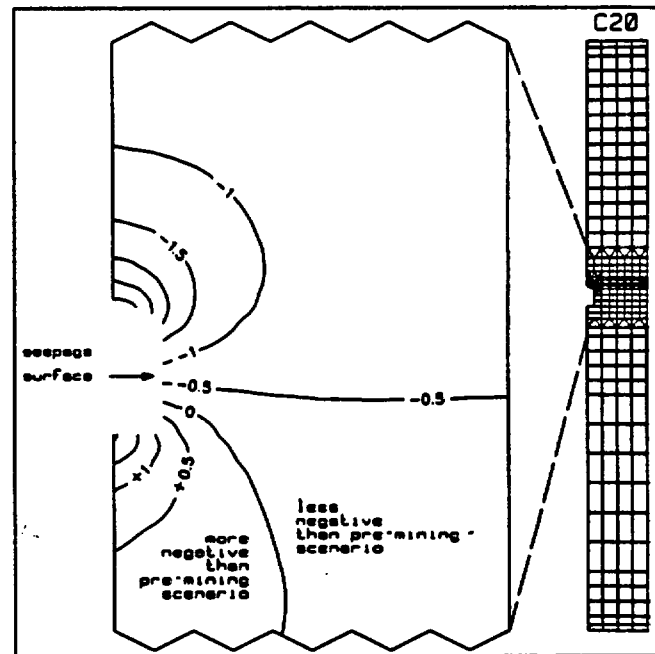


Fig. 7 — Change in pressure caused by a drift (seepage surface) (Intervals of pressure head change = 0.5 m (1.6 ft), flux = 0.44 mm/a (0.017 in. per year; see Fig. 4 for scale).

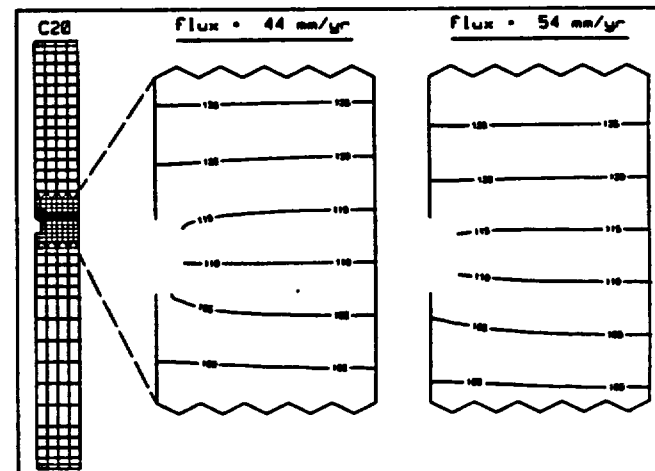


Fig. 8 — Prototype equipotential maps for flux values of 0.44 and 0.54 mm/a (0.017 and 0.02 in. per year) (equipotentials in meters). Not to scale.

0.44 mm/a (0.017 in. per year) and 0.5 m (1.6 ft) for a flux of 0.54 mm/a (0.02 in. per year).

Flow through mesh C20 is affected by a drift that is incorporated as a seepage boundary as shown in Figs. 7 and 8. The effect on the distribution of pressure head is to increase pressures above and adjacent to the drift and to decrease pressures in the area immediately beneath the seepage boundary. In the vicinity of the drift, pressures are least negative along its upper edge. The decrease in cross-sectional area available for capillary flow causes the pressure changes relative to the pre-mined case.

The effect of the drift on the ground water flow pattern depends on the magnitude of flux, as shown in Fig. 9. The drift acts as an impermeable barrier to flow at low values of flux. Non-horizontal lines of equal potential indicate a horizontal component to the velocity vector. At higher values of flux, atmospheric pressure develops at nodes that define the upper edge of the drift. In this case, some flow is diverted around the rock-drift interface, and some flow exits the flow system as mine water inflow.

Mine water inflow

Mine water inflow as a function of mine design variables and flux is presented in Table 3. To facilitate comparison, mine water inflow rates are expressed both in raw form and as percentages of the flux at the constant flux, upper boundary. The percentage is calculated as follows:

$$\% = 100 \times \Sigma I / (H \times F)$$

where ΣI = sum of the nodal mine water inflow rates,
 H = horizontal dimension of seepage surface, and
 F = flux at constant-flux, upper boundary.

The denominator represents the downward flux through the

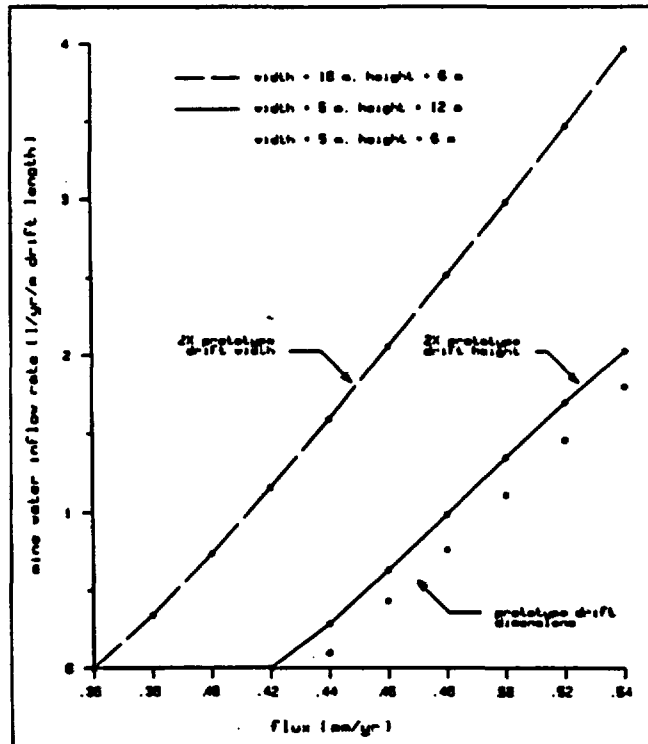


Fig. 9 — Comparison of the effect on mine water inflow rate of doubling the drift width with doubling the height (drift spacing = 40 m (131 ft), drift back slope = 0°).

width of material replaced by the seepage boundary (the drift), except Fig. 11, where it is the total width of the mesh.

All of the design variables tested affect the rate of mine water inflow. The mine water inflow rate increases with the dimensions of the drifts and with the magnitude of the flux. The mine water inflow rate decreases with increasing drift back slope. The influence of drift spacing decreases with increasing magnitude of spacing.

The effects of mine design geometry on the rate of mine water inflow are shown graphically in Figs. 9 through 13. A comparison of the effects of drift height and drift width, the two most influential design variables, is shown in Fig. 9. Each of Figs. 10 through 13 illustrates the effect of a different design variable over a range of flux values.

Figure 9 shows that doubling the horizontal dimension of a

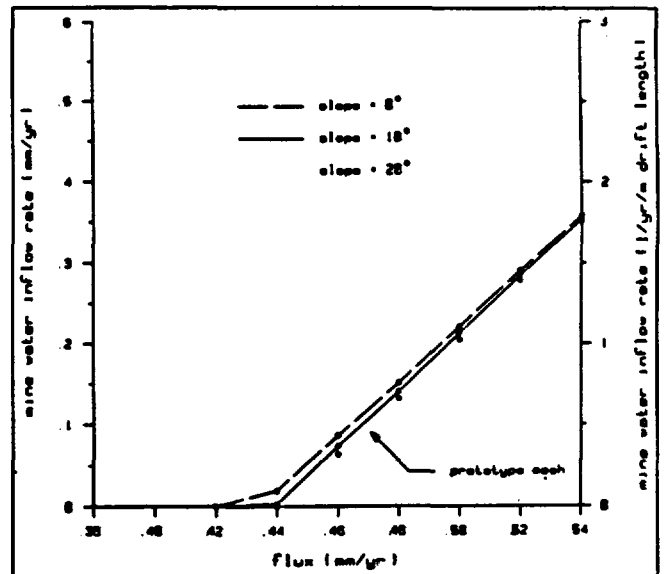


Fig. 10 — Mine water inflow rate as a function of drift back slope and flux (drift spacing = 40 m or 131 ft, drift width = 5 m or 16 ft, drift height = 6 m or 19.6 ft).

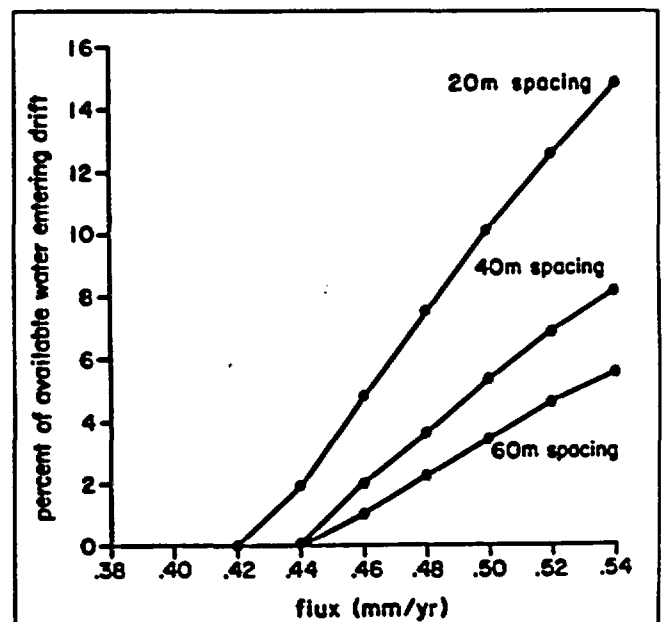


Fig. 11 — Mine water inflow rate as a function of drift spacing and flux (drift width = 5 m or 16 ft, drift height = 6 m or 19.6 ft, drift back slope = 20°).

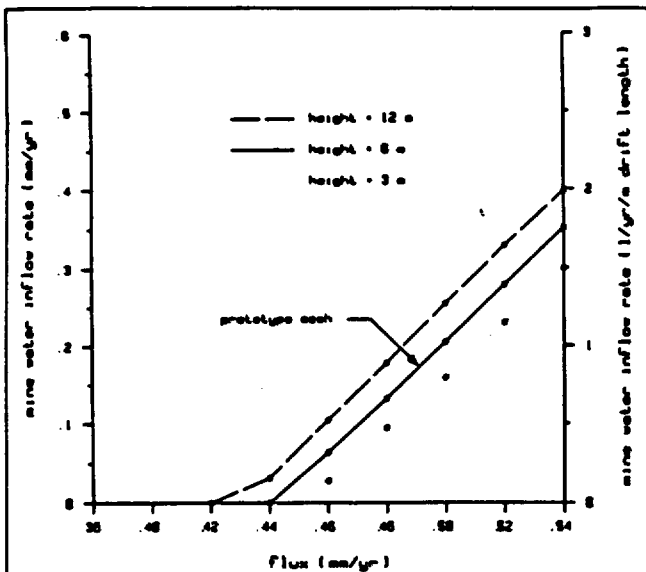


Fig. 12 — Mine water inflow rate as a function of drift height and flux (drift spacing = 40 m 131 ft, drift width = 5 m or 16 ft, drift back slopes = 20°).

drift or room has a far greater effect on the rate of mine water inflow than does doubling the vertical dimension.

The effect of drift spacing is shown in Fig. 11. The vertical axis in this figure is the percent of total flux that enters the drift. As would be expected, this percentage increases with increased flux but decreases with increased spacing. The actual amount of water entering the drift is equal to the spacing times the flux times the percentage and is about the same for 40 and 60 m (131 and 197 ft) spacing. This simulation shows that some optimal spacing exists above which inflow does not depend on spacing. Increasing the spacing further would have minimal effect on the predicted mine water inflow rate if all other input variables remained unchanged.

When mine design geometry is fixed, the relationship between inflow rate and flux is very nearly linear above a critical value of flux (Figs. 9-13). The critical flux corresponds to the development of atmospheric pressure at one or more nodes comprising the seepage boundary of the drift.

An atmospheric pressure condition occurs for all simulated mine designs at values of flux appreciably less than the saturated hydraulic conductivity of the mesh material (Table 3). Mine

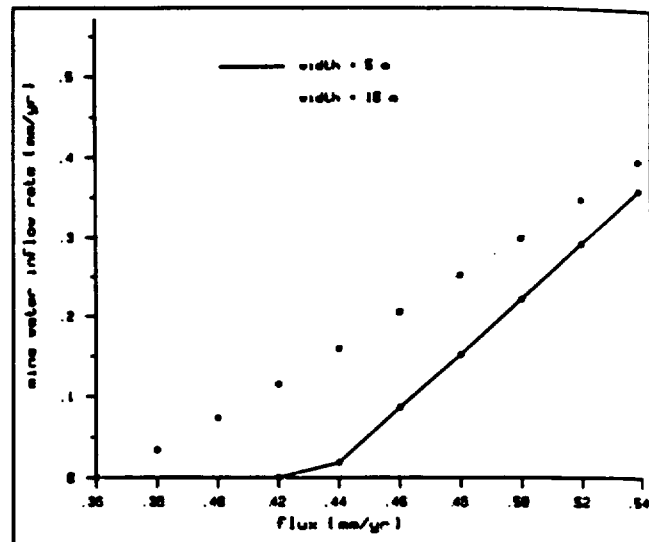


Fig. 13 — Mine water inflow rate as a function of drift width and flux (drift spacing = 40 m or 131 ft, drift height = 6 m or 19.6 ft, drift back slope = 0°).

water inflow occurs at the lowest flux with the design shown in mesh G of Fig. 4. The seepage boundary that corresponds to the drift in mesh G is twice the width of the other drifts.

Conclusions

The design and development of a mine in unsaturated rock, such as the Topopah Spring Tuff at Yucca Mountain, NV, will affect the movement of water in the unsaturated zone. Modeling results presented here indicate that mining-induced changes to ground water flow are site specific and design dependent.

Variables of influence include mine design geometry and the nature of the pre-mining ground water flow system. Conclusions derived from this study are:

- The creation of a mined-out opening reduces the cross-sectional area of rock available for unsaturated flow. A general pressure increase and saturation level increase result.
- The effect of a mined-out opening on ground-water flow in the vadose zone depends on the pressure condition at the interface of the mine with the host rock. The opening is impermeable to liquid water if the pressure at that boundary is less than atmospheric. In such a case, a horizontal component to the flow

Table 3 — Rates of mine water inflow at steady state [sds = simulated drift spacing; sdh = simulated drift height; sdw = simulated drift width; dbs = drift back slope].

flux (mm/yr)	mesh B0 sds = 20 m sdh = 6 m sdw = 6 m dbs = 0°	mesh B10 sds = 20 m sdh = 6 m sdw = 6 m dbs = 10°	mesh B20 sds = 20 m sdh = 6 m sdw = 6 m dbs = 20°	mesh C0 sds = 40 m sdh = 6 m sdw = 6 m dbs = 0°	mesh C10 sds = 40 m sdh = 6 m sdw = 6 m dbs = 10°	mesh C20 sds = 40 m sdh = 6 m sdw = 6 m dbs = 20°	mesh D0 sds = 60 m sdh = 6 m sdw = 6 m dbs = 0°	mesh D10 sds = 60 m sdh = 6 m sdw = 6 m dbs = 10°	mesh D20 sds = 60 m sdh = 6 m sdw = 6 m dbs = 20°
0.54	3.26 x 10 ⁻¹ (60.4)**	3.23 x 10 ⁻¹ (59.8)	3.20 x 10 ⁻¹ (59.2)	3.58 x 10 ⁻¹ (66.4)	3.54 x 10 ⁻¹ (65.5)	3.51 x 10 ⁻¹ (65.0)	3.66 x 10 ⁻¹ (67.8)	3.62 x 10 ⁻¹ (67.0)	3.59 x 10 ⁻¹ (66.5)
0.52	2.70 x 10 ⁻¹ (51.9)	2.66 x 10 ⁻¹ (51.1)	2.62 x 10 ⁻¹ (50.3)	2.91 x 10 ⁻¹ (56.0)	2.85 x 10 ⁻¹ (54.6)	2.79 x 10 ⁻¹ (53.7)	2.98 x 10 ⁻¹ (57.3)	2.91 x 10 ⁻¹ (56.0)	2.85 x 10 ⁻¹ (54.9)
0.50	2.12 x 10 ⁻¹ (42.4)	2.07 x 10 ⁻¹ (41.4)	2.02 x 10 ⁻¹ (40.3)	2.21 x 10 ⁻¹ (42.6)	2.13 x 10 ⁻¹ (42.6)	2.05 x 10 ⁻¹ (41.0)	2.25 x 10 ⁻¹ (44.9)	2.16 x 10 ⁻¹ (43.2)	2.07 x 10 ⁻¹ (41.3)
0.48	1.56 x 10 ⁻¹ (32.4)	1.48 x 10 ⁻¹ (30.8)	1.43 x 10 ⁻¹ (29.9)	1.51 x 10 ⁻¹ (31.5)	1.40 x 10 ⁻¹ (29.2)	1.32 x 10 ⁻¹ (27.6)	1.51 x 10 ⁻¹ (31.4)	1.38 x 10 ⁻¹ (28.7)	1.29 x 10 ⁻¹ (27.0)
0.46	1.04 x 10 ⁻¹ (22.5)	9.48 x 10 ⁻² (20.6)	8.87 x 10 ⁻² (19.3)	8.61 x 10 ⁻² (18.7)	7.31 x 10 ⁻² (15.9)	6.33 x 10 ⁻² (13.8)	8.21 x 10 ⁻² (17.8)	6.74 x 10 ⁻² (14.7)	5.62 x 10 ⁻² (12.2)
0.44	5.13 x 10 ⁻² (11.7)	4.13 x 10 ⁻² (9.38)	3.37 x 10 ⁻² (7.86)	1.90 x 10 ⁻² (4.33)	2.80 x 10 ⁻² (0.591)	0	1.03 x 10 ⁻² (2.34)	0	0
0.42	4.06 x 10 ⁻² (0.966)	0	0	0	0	0	0	0	0
0.40	0	0	0	0	0	0	0	0	0

* mine water inflow rate in millimeters per year.

** mine water inflow rate expressed as a percentage of the constant flux.

velocity vector results. Inflow of water to the mined out opening occurs if the pressure condition reaches atmospheric.

- Mine water inflow is possible from the initially unsaturated zone, even for mines developed in homogeneous rock. Moreover, mine water inflow can occur at values of downward flux appreciably less than the saturated hydraulic conductivity of the host rock.

- The theoretical rate of mine water inflow is proportional to the magnitude of the flux. The relationship is approximately linear above the critical value of flux, where the critical value is defined as the minimum value for which an atmospheric pressure condition occurs at the drift-rock interface.

- The theoretical rate of mine water inflow depends on mine geometry. The rate of mine water inflow increases with drift dimensions and is affected by drift spacing. The influence of drift spacing decreases with increasing magnitude of spacing. Mine water inflow rates are greatest for mine openings with horizontal backs (roofs). Drift width is the mine design variable that has the greatest effect on the per drift rate of mine water inflow in unsaturated rocks. Ground water inflow rate into a repository in the unsaturated zone would be minimized by a mine design that stipulates tall, narrow drifts.

- The requisite condition for mine water inflow is atmospheric pressure on the water at the drift-rock interface. The mechanism of mine water inflow is analogous to the theory for flow entering an open fracture; only the scales are different. Consequently, the qualitative aspects of the results of this study are relevant to the study of flow affected by discrete, open fractures. Under this analogy, if all other variables are held constant, the lower the dip of the fracture the greater is the probability of positive pressure in it.

- With reference to Yucca Mountain, if the spatial average

downward flux is the 0.5 mm/a (0.02 in. per year) used by Montazer and Wilson (1984) (or greater), and if the permeability values presented by Montazer and Wilson (1984) are representative, it is probable that the inflow of water into the mined out repository cannot be avoided using the current design. ♦

References

- Bloomsburg, G.L., Williams, R.E., and Osiensky, J., 1989, "Distribution of downward flux in unsaturated heterogeneous hydrogeology environments." *Geological Society of America Bulletin*, Vol. 101, No. 2.
- Coney, A.T., 1985, "Mechanics of immiscible fluids in porous media." Water Resources publications, Littleton, CO, 255 p.
- Davis, L.A., and Neuman, S.P., 1983, "Documentation and user's guide: UNSAT2 variably saturated flow model." Prepared for Division of Waste Management, US Nuclear Regulatory Commission, NUREG/CR-3390.
- MacDougall, H.R., 1984, "Two-stage repository development at Yucca Mountain: An engineering feasibility study." Sandia National Laboratories, Albuquerque, NM, SAND84-1351.
- Montazer, P., and Wilson, W.E., 1984, "Conceptual hydrologic model of flow in the unsaturated zone, Yucca Mountain, NV." US Geological Survey, Lakewood, CO, Water Resources Investigations Report, USGS-WRI-844345.
- Mualem, Y., 1976, "A new model for predicting the hydraulic conductivity of unsaturated porous materials." *Water Resources Research*, Vol. 13, No. 3, pp. 513-522.
- Peters, R.R., et al., 1984, "Fracture and matrix hydrologic characteristics of tuffaceous materials from Yucca Mountain, Nye County, NV." Sandia National Laboratories, Albuquerque, NM, SAND84-1471.
- US Department of Energy, 1986, Environmental Assessment, Yucca Mountain Site, Nevada Research and Development Area, Nevada. DOE/RW-0073, Washington, DC.
- van Genuchten, R., 1980, "A closed-form equation for predicting the hydraulic conductivity of unsaturated soils." *Journal of the Soil Sciences Society of America*, Vol. 44, pp. 892-898.
- Vincent, S.D., 1989, "Application of a ground water flow model to the hydrogeologic impacts of mine development in unsaturated rock, MS thesis, Department of Geology and Geological Engineering, College of Mines and Earth Resources, University of Idaho, Moscow, ID.
- Williams, R.E., et al., 1986, *Mine Hydrology*, SME, Inc., Littleton, CO, p.169.
- Zamal, M., 1968, "On the finite element method." *Numerical Mathematics*, Vol. 12, p. 394-4*9.